

Title	Inner nuclear membrane proteins Lem2 and Bqt4 interact with different lipid synthesis enzymes in fission yeast
Author(s)	Hirano, Yasuhiro; Kinugasa, Yasuha; Kubota, Yoshino et al.
Citation	Journal of Biochemistry. 2023, 174(1), p. 33-46
Version Type	AM
URL	https://hdl.handle.net/11094/92448
rights	© 2023 Oxford University Press. Published by Oxford University Press on behalf of the Japanese Biochemical Society. All rights reserved.
Note	

Osaka University Knowledge Archive : OUKA

<https://ir.library.osaka-u.ac.jp/>

Osaka University

Inner nuclear membrane proteins Lem2 and Bqt4 interact with different lipid synthesis enzymes in fission yeast

Yasuhiro Hirano^{1,*}, Yasuha Kinugasa¹, Yoshino Kubota¹, Chikashi Obuse², Tokuko Haraguchi¹ and Yasushi Hiraoka^{1,*}

¹Graduate School of Frontier Biosciences, Osaka University, Suita 565-0871, Japan;

²Graduate School of Science, Osaka University, Toyonaka, Osaka 560-0043, Japan

Running title: Proteomic analysis of Lem2 and Bqt4-binding proteins

*** Corresponding to:**

Yasuhiro Hirano (yhira@fbs.osaka-u.ac.jp) and Yasushi Hiraoka (hiraoka@fbs.osaka-u.ac.jp), Graduate School of Frontier Biosciences, Osaka University, 1-3 Yamadaoka, Suita 565-0871, Japan. Tel.: +81-6-6879-4621, FAX: +81-6-6789-4622

1 **Summary**

2 The nuclear envelope (NE) is a double-membrane structure consisting of inner and outer membranes that
3 spatially separate the nucleus from the cytoplasm, and its function is critical for cellular functions, such as
4 genome maintenance. In the fission yeast, *Schizosaccharomyces pombe*, the inner nuclear membrane
5 proteins, Lem2 and Bqt4, play pivotal roles in maintaining the NE structure. We previously found that the
6 double deletion of *lem2*⁺ and *bqt4*⁺ causes a synthetic lethal defect associated with severe NE rupture, and
7 overexpression of Elo2, a solo very-long-chain fatty acid elongase, suppresses this defect by restoring the
8 NE. However, the molecular basis of this restoration remains elusive. To address this, we identified
9 Lem2- and Bqt4-binding proteins via immunoprecipitation and mass spectrometry in this study. Forty-
10 five and 23 proteins were identified as Lem2- and Bqt4-binding proteins, respectively. Although these
11 binding proteins partially overlapped, Lem2 and Bqt4 interacted with different types of lipid metabolic
12 enzymes: Cho2, Ole1, and Erg11 for Lem2 and Cwh43 for Bqt4. These enzymes are known to be
13 involved in various lipid synthesis processes, suggesting that Lem2 and Bqt4 may contribute to the
14 regulation of lipid synthesis by binding to these enzymes.

15

16

17 **Keywords:** nuclear envelope, Lem2, Bqt4, *Schizosaccharomyces pombe*, proteome analysis

18

19

20 **Introduction**

21 The nuclear envelope (NE) is a double-membrane structure that acts as a physical barrier to spatially
22 separate the genomic DNA from the cytoplasm. The NE comprises the outer nuclear membrane (ONM)
23 and inner nuclear membrane (INM). ONM contains many NE-specific integral membrane proteins and
24 shares many integral membrane proteins with the endoplasmic reticulum (ER) due to its continuity with
25 the ER. In contrast, INM is enriched in only NE-specific integral membrane proteins, many of which are
26 thought to play important roles in the interactions of the NE with chromatin (1). These interactions
27 modulate the genetic activities of chromosomes via the formation of heterochromatin beneath the NE (2-
28 4). INM and ONM are joined at the nuclear pore complex (NPC), forming a pore structure that penetrates
29 the nuclear envelope. Material transport between the nucleus and cytoplasm occurs via the NPC. The NE
30 plays an essential role in genomic activities, such as replication and transcription, by regulating chromatin
31 structures and nucleocytoplasmic transport, and the rupture or opening of NE causes genomic instability
32 and subsequent cell death (5, 6). Therefore, structural maintenance of the NE is crucial for cell viability
33 (7).

34 To date, several hundreds of INM proteins have been identified in vertebrates via proteomic
35 analysis (8-10). Among them, the LEM (Lap2–emerin–Man1) domain protein, Lem2, is one of the most
36 characterized NE proteins that is well conserved among various species, including *Tetrahymena*, yeast,
37 and humans (11-14). Lem2 contributes to nuclear reformation during mitosis by promoting membrane
38 fusion mediated by the ESCRT-III complex in human cells (15, 16). Similarly, in budding and fission
39 yeasts, Lem2 recruits Chm7/Cmp7 (CHMP7 in humans) and other ESCRT-III components to the ruptured
40 sites of the NE to seal it at the end of mitosis (15-19). In addition to these cooperative functions with the
41 ESCRT-III complex, Lem2 has been reported to be involved in various nuclear processes, such as
42 heterochromatin formation (20-22), exosome-mediated RNA elimination (23), and NE/ER boundary
43 formation, with the ER protein, Lnp1 (homolog of human Lunapark), in the fission yeast,
44 *Schizosaccharomyces pombe* (24, 25).

45 The most striking phenotype derived from Lem2 is that depletion of Lem2, but not Man1
46 (another LEM-domain protein), confers synthetic lethality with depletion of Bqt4 in association with
47 nuclear membrane rupture (6, 22, 26), suggesting that Lem2 and Bqt4 play crucial roles in the
48 maintenance of NE integrity. Bqt4 is a tail-anchored INM protein that is conserved in the
49 *Schizosaccharomyces* genus and was originally found to anchor telomeres to the NE via its association
50 with the telomere protein, Rap1, during vegetative growth (27). Bqt4 also plays an important role in
51 telomere clustering during meiosis, together with the meiosis-specific Bqt1-Bqt2 complex that bridges
52 telomeres to the NE (27, 28). However, the role of Bqt4 in NE maintenance, independent of telomere
53 anchoring, remains unclear.

54 In a previous study, we identified Elo2 as a suppressor of the synthetic lethality of Lem2 and
55 Bqt4 double-depletion mutants (6). Elo2 is a solo very-long-chain fatty acid elongase in *S. pombe* that
56 generates very long-chain (over C24) fatty acids that are eventually incorporated into ceramide species.
57 Overexpression of Elo2 restores ceramide levels and suppresses the nuclear membrane rupture phenotype
58 in the Lem2 and Bqt4 double-depletion mutant (6), suggesting that Lem2 and Bqt4 cooperatively
59 participate in nuclear membrane homeostasis. However, the molecular basis for this restoration remains
60 unclear, although Lem2-binding partners have been identified using a membrane yeast two-hybrid assay
61 (29). In this study, we attempted to identify the binding proteins of Lem2 and Bqt4 via
62 immunoprecipitation (IP) and subsequent mass spectrometry (MS).

63

64 **Materials and methods**

65 **Yeast strains and media**

66 *S. pombe* strains used in this study are listed in Supplementary Table 1. Cells were cultured at 30 °C. For
67 the routine maintenance of *S. pombe* cells, a rich medium containing yeast extract with supplements (YES)
68 was used (30). As a minimum medium, Edinburgh minimal medium with 5 mg/mL glutamate instead of
69 NH₄Cl (EMMG) or EMMG5S (EMMG with 0.225 mg/mL adenine, leucine, uracil, lysine, and histidine)

70 was used. Cell strains carrying *lem2*Δ were maintained in EMMG to avoid genomic instability, which occurs
71 in rich medium, as previously reported (6, 22, 24, 26). To select *S. pombe* cells carrying *kan^r*, *hph*, *NAT*,
72 and *aur1^r* genes as selection markers, cells were cultured for 2–4 d on YES plates containing 100 μg/mL
73 G418 disulfate (Nacalai Tesque, Kyoto, Japan), 200 μg/mL hygromycin B (FUJIFILM Wako Pure Chemical
74 Corp., Osaka, Japan), 100 μg/mL nourseothricin sulfate (WERNER BioAgents, Jena, Germany), and 100
75 μg/mL blasticidin S (FUJIFILM Wako Pure Chemical Corp.), respectively.

76

77 **Plasmid construction**

78 All plasmids used in this study were constructed using In-Fusion (Takara Bio Inc., Kusatsu, Japan; Cat.
79 #639648) and NEBulider (New England Biolabs, Ipswich, USA; Cat. #E2621L), according to the
80 manufacturer's protocol. The plasmid encoding FLAG-Lem2-HA was constructed as previously described
81 (26). To generate the plasmid encoding FLAG-Bqt4-HA for expression, the coding sequence of *bqt4⁺* was
82 amplified via PCR and inserted into the pCST4-FLAGHA vector between *Bam*HI and *Bg*III sites.

83

84 **Gene disruption, integration, and tagging**

85 Gene disruption, integration, and tagging were performed using a two-step PCR method for direct
86 chromosome integration, as previously described (31, 32). Briefly, for the first-round PCR, ~500 bp
87 genomic sequences upstream and downstream from the open reading frames (ORFs) of interest were
88 amplified via PCR using KOD One (TOYOBO, Osaka, Japan; Cat. #KMM-201). These PCR products were
89 then used as primers for second-round PCR to amplify a template sequence containing the selection markers.
90 The resulting PCR products were transformed into *S. pombe* cells for disruption, integration, and tagging,
91 and transformants were selected on an appropriate selection plate. The obtained strains were confirmed for
92 correct constructions of disruption, integration, and tagging via genomic PCR using KOD Fx Neo
93 (TOYOBO; Cat. #KFX-201) at the 5' and 3' ends of the target gene. In addition, we performed genomic
94 PCR inside the ORF of the target gene to confirm the absence of an ORF in the genome.

95

96 **Immunoprecipitation (IP)**

97 *S. pombe* cells harboring a gene encoding FLAG-Lem2-HA or FLAG-Bqt4-HA for expression under the
98 control of the *nmt1* promoter were pre-cultured in EMMG supplemented with 10 μ M thiamine, followed
99 by incubation in EMMG without thiamine for 17 h at 30 °C to induce protein expression.

100 For one-step purification to prepare samples 1 and 2 in Fig. 1B, cells (5.0×10^7) were
101 resuspended in 100 μ L CSK-HEPES buffer (10 mM HEPES-NaOH pH7.4, 3 mM $MgCl_2$, 300 mM
102 sucrose, 1 mM EDTA, and 0.5% Triton X-100 containing either 150 mM or 300 mM NaCl) supplemented
103 with 2 mM phenylmethylsulfonyl fluoride and 5% protease inhibitor cocktail (P8215; Sigma-Aldrich,
104 USA) and homogenized with Multi-Beads Shocker (Yasui Kikai, Co., Japan) at 2,700 rpm for 10 cycles
105 of 60 s on and 60 s off. Cell homogenates were centrifuged, and the supernatants were diluted to five
106 times their volume with CSK-HEPES buffer to prepare the cell extract. The cell extract was incubated
107 with 100 ng of anti-HA rat monoclonal antibody (3F10; Roche, Switzerland) and 30 μ L of Dynabeads
108 sheep anti-rat IgG (11035; Thermo Fisher Scientific Inc., USA) for 3 h at 4°C. Dynabeads were washed
109 five times to remove the non-specific bound proteins. Specific bound proteins were eluted with the
110 Laemmli sodium dodecyl sulfate (SDS) sample buffer (62.5 mM Tris-HCl pH6.8, 2% SDS, 10% glycerol
111 and 0.0025% bromophenol blue).

112 For two-step purification to prepare samples 3 and 4 in Fig. 1B, cells (1.0×10^8 and 1.6×10^9 for
113 Lem2 and Bqt4, respectively) were suspended in CSK-Tris buffer (20 mM Tris-HCl pH8.0, 150 mM
114 NaCl, 3 mM $MgCl_2$, 300 mM sucrose, 1 mM EDTA, and 0.5% Triton X-100) and homogenized as
115 described above. The cell extract was incubated with anti-FLAG M2 beads (A2220; Sigma-Aldrich,
116 USA) for 2 h at 4°C. After removing the non-specific bound proteins by washing the beads five times, the
117 bound proteins were eluted with CSK-Tris buffer containing 100 μ g/mL of 3 \times FLAG peptide (F4799;
118 Sigma-Aldrich, USA). The eluate was incubated with 100 ng of anti-HA rat monoclonal antibody (3F10)
119 and 30 μ L of Dynabeads sheep anti-rat IgG for 2 h at 4°C. To remove the non-specific bound proteins, the

120 beads were washed five times with CSK-Tris buffer. Then, specifically bound proteins were eluted with
121 0.1 M glycine-HCl (pH 2.5), followed by neutralization with 1 M Tris-HCl (pH8.0). One tenth of the
122 eluate was subjected to silver staining (SilverQuest, Invitrogen, Waltham, USA) to determine the amount
123 of protein in the eluate using bovine serum albumin (BSA) as the standard and the remaining nine tenths
124 were used for MS analysis.

125

126 **Mass spectrometry (MS)**

127 MS was performed according to a previously described procedure (33, 34). Detected peptides were
128 searched against the PomBase protein dataset released on November 12, 2015.

129

130 **Classification by gene ontology (GO)**

131 Classification of proteins by GO was based on the PomBase database (<https://www.pombase.org/>;
132 accessed on October 13, 2022) (35). Fold enrichment of the GO-slim term was calculated as follows: the
133 percentage of proteins classified into each GO-slim term out of the total identified proteins was calculated
134 and divided by the percentage of those calculated from all records in the PomBase database.

135

136 **Western blotting (WB)**

137 Samples were prepared using a two-step purification method, as described in the IP section, and subjected
138 to 10% SDS-PAGE. After electrophoresis, the proteins were transferred onto polyvinylidene difluoride
139 membranes. GFP-tagged proteins were probed with an anti-GFP polyclonal antibody (0.5 µg/mL, 1:2,000
140 dilution; Rockland Inc., Philadelphia, PA, USA; Cat #600-401215). FLAG-Lem2-HA and FLAG-Bqt4-
141 HA were probed with an anti-HA monoclonal antibody (1:2,000 dilution; 3F10). Protein bands were
142 detected using chemiluminescence (ImmunoStar LD or Zeta; FUJIFILM Wako Pure Chemical Corp.; Cat
143 #296-69901 and #297-72401).

144

145 Indirect immunofluorescence staining

146 Indirect immunofluorescence staining was performed according to a previously described procedure (36)
147 except that anti-HA rat monoclonal (1:100 dilution; 3F10) and Alexa488-labeled anti-rat IgG (1:250
148 dilution; Thermo Fisher Scientific) antibodies were used as primary and secondary antibodies,
149 respectively.

150

151 Live cell imaging

152 Subcellular localization of GFP-S65T (designated as “GFP” throughout this manuscript) fusion proteins
153 was observed in living cells. Cells were cultured overnight in EMMG at 30°C to attain the logarithmic
154 growth phase before placing them onto a glass-bottom dish (MatTek, Ashland, USA; Cat. #P35G-1.5-14-
155 C). Cells were attached to glass via soybean lectin (Sigma-Aldrich, St. Louis, USA; Cat. #L1395) and
156 covered with EMMG.

157

158 Fluorescence microscopy

159 *S. pombe* cells were observed using the DeltaVision Elite system (GE Healthcare Inc., Chicago, USA)
160 equipped with pco.edge 4.2 sCMOS (PCO, Kelheim, Germany) or CoolSNAP HQ2 cooled-CCD camera
161 (Photometrics, Tucson, USA); the 60× PlanApo N OSC oil-immersion objective lens (numerical aperture
162 [NA] = 1.4, Olympus, Tokyo, Japan) objective lens was used. Optical section images were acquired at 0.2
163 μm intervals. All images were deconvolved using the built-in SoftWoRx software (v7.0.0) using the
164 default setting with a homemade optical transfer function. Excitation intensity and exposure time were
165 adjusted for each condition as the expression levels of the proteins were different. The brightness of
166 images was linearly changed using Fiji software (v1.53t) (37) for better visibility.

167

168 Results and Discussion**169 Lem2 interacts with lipid synthesis enzymes**

170 To identify Lem2-binding proteins, we first generated *S. pombe* cells expressing Lem2 tagged with FLAG
171 and HA in the N-terminus and C-terminus, respectively (FLAG-Lem2-HA), or tags-only (FLAG-HA) as a
172 control. Indirect immunofluorescence staining of the cells showed that the FLAG-Lem2-HA protein was
173 localized in NE, whereas FLAG-HA as a control was not (Fig. 1A). This NE localization of FLAG-Lem2-
174 HA is consistent with the previously reported localization of Lem2-GFP (12, 38). Based on this
175 localization pattern, we determined that FLAG-Lem2-HA was sufficient to identify the Lem2-binding
176 proteins. Thus, IP was performed on FLAG-Lem2-HA.

177 We tested four different IP conditions (samples #1–4; Fig. 1B). First, we performed one-step
178 purification: Lem2-binding proteins were immunoprecipitated using an anti-HA antibody at 150 or 300
179 mM NaCl (samples #1 and #2, Fig. 1B). Specific bands were observed with both 150 and 300 mM NaCl
180 in the Lem2 precipitant compared to the control, indicating that our IP procedure effectively enriched the
181 Lem2-binding proteins. Some of the binding proteins observed under the 150 mM NaCl condition
182 remained bound under the 300 mM NaCl condition, suggesting that these proteins may bind to Lem2
183 more tightly than others (sample #2 in Fig. 1B). Next, we performed two-step purification: Lem2 binding
184 proteins were first immunoprecipitated using anti-FLAG and then immunoprecipitated using anti-HA
185 antibodies (samples #3 and #4, Fig. 1B). We investigated whether endogenous Lem2 antagonized the
186 interaction between FLAG-Lem2-HA and its binding proteins and found no obvious differences in the
187 presence or absence of endogenous Lem2 (samples #3 and #4 in Fig. 1B).

188 Analysis of these four samples via liquid chromatography (LC)/MS led to the identification of
189 45 proteins; eight out of 45 proteins (Bqt4, Cho2, Ole1, Nmd5, Erg11, Ape2, Rad25, and Rpl6) were
190 detected in all four conditions, and the remaining 37 proteins (including Vtc4) were detected in all
191 conditions, except the 300 mM NaCl condition (Table 1). Bqt4, Ole1, and Vtc4 have been reported as
192 Lem2-binding proteins via IP–WB analysis and yeast-two-hybrid assays (26, 29); however, some of the
193 known Lem2-binding proteins, such as Nur1 (21) and Sad1 (12), were not detected under any of the four
194 conditions tested in this study. This result suggests that most, if not all, of the proteins identified in this

195 study were Lem2-binding proteins. Furthermore, some Lem2-binding proteins, such as Cho2 and Erg11,
196 were found to be involved in lipid metabolism.

197 Next, we classified the 45 binding proteins according to GO terms (Table 1 and Fig. 1C). GO
198 classification revealed that the enriched proteins were related to lipid metabolism (Cho2, Ole1, Erg11,
199 Hmg1, Fas1, Erg5, Tsc13, Lef1, and Its8; fold enrichment [FE] = 3.81), nucleocytoplasmic transport
200 (Nmd5, Kap123, and Sal3; FE = 2.97), protein folding (Cct3, Hsp90, and SPBC17A3.05c; FE = 3.59),
201 and protein glycosylation (Wbp1, Stt3, and Ost1; FE = 4.48). Notably, proteins involved in N-
202 glycosylation and folding were enriched together with Bip1, a member of the Hsp70 family, implying that
203 Lem2 participates in protein quality control. Enrichment of the karyopherin/importin β family is
204 convincing as karyopherin/importin β mediates the nuclear import of Heh1/Lem2 in *Saccharomyces*
205 *cerevisiae* (39). Proteins related to lipid metabolism control membrane homeostasis cooperatively with
206 Lem2, as Lem2 is involved in nuclear membrane maintenance in cooperation with Bqt4 (22, 26) and with
207 Elo2, a very-long-chain fatty acid elongase (6). We selected Cho2, Ole1, and Erg11 identified under 300
208 mM NaCl as Lem2-binding proteins and further evaluated their interactions with Lem2 via IP–WB.
209 GFP-tagged Cho2 (GFP-Cho2), Ole1 (GFP-Ole1), and Erg11 (Erg11-GFP) were expressed in *S. pombe*
210 expressing FLAG-Lem2-HA. GFP alone, instead of GFP-tagged proteins, was expressed in cells as a
211 control. After cell lysis, IP was performed on the cell lysates using an anti-HA antibody. The proteins
212 obtained via IP were further analyzed via WB using anti-GFP or anti-HA antibodies (Fig. 2A). All three
213 proteins, Cho2, Ole1, and Erg11, were detected using an anti-GFP antibody (see “WT” in Fig. 2A). This
214 result is consistent with the IP–MS results. Next, we examined whether Bqt4 mediated these interactions
215 because Lem2 binds to Bqt4 and its NE localization depends on Bqt4 (26). We performed an IP–WB
216 experiment on the *bqt4* Δ background (“*bqt4* Δ ” in Fig. 2A). Deletion of *bqt4*⁺ did not affect these
217 interactions, indicating that Cho2, Ole1, and Erg11 interact with Lem2 independent of Bqt4. Finally, we
218 examined whether Lem2 affected their subcellular localization. GFP-Cho2, GFP-Ole1, and Erg11-GFP
219 were localized in the cortical ER and NE (or perinuclear ER), and deletion of the *lem2*⁺ gene did not

220 affect their localization (Fig. 2B), indicating that Lem2 is not necessary for the NE localization. As Cho2,
221 Ole1, and Erg11 function in the synthesis of phosphatidylcholine, unsaturated fatty acids, and ergosterol,
222 respectively, Lem2 potentially plays a broad role in regulating the lipid composition of the nuclear
223 membrane.

224

225 **Bqt4 interacts with lipid synthesis enzymes different from those of Lem2**

226 We attempted to identify Bqt4-binding proteins because our previous analyses demonstrated a functional
227 relationship between Lem2 and Bqt4 (6, 22, 26). FLAG-Bqt4-HA was expressed in *S. pombe* cells. Using
228 this strain, Bqt4-binding proteins were immunoprecipitated using a two-step purification method in two
229 independent experiments and analyzed via LC/MS (Fig. 3A, B). Twenty-three proteins were identified in
230 both replicates (Fig. 3B and Table 2). Our analyses detected only one known Bqt4-binding protein, Imp1
231 (40), whereas other known binding proteins, such as Bqt3 (27) and Lem2 (26), were not detected via
232 LC/MS. To examine whether Bqt3 and Lem2 were present in the IP fractions, we performed WB and
233 detected both Bqt3 and Lem2 in the IP fractions (Fig. 3C), demonstrating the validity of our IP fractions.
234 Bqt3 and Lem2 were not detected via MS possibly due to their property or abundance. Furthermore, Bqt3
235 is a small protein with almost the entire sequence composed of transmembrane domains, which may limit
236 the number of observable peptides in MS analysis. In case of Lem2, the expression level of Lem2 seems
237 to be lower than that of Bqt4, according to the PomBase database. Consistent with this, over half of the
238 Lem2-binding proteins (24 out of 45 proteins) were detected as minor Bqt4-binding proteins (see yellow-
239 highlighted sections in Supplementary Table S2).

240 APSES domain of Bqt4 has been reported to function as an interaction surface for protein
241 binding and one consensus binding motif of the domain is (D/E)₃₋₄XFXXX ϕ , where ϕ represents
242 hydrophobic amino acids (41). This motif was found in 96 proteins in *S. pombe* by Pombase database
243 search, but only Bip1 had this motif at its C-terminal end (652-DDDYFDDEA-660) among the 23
244 identified Bqt4-binding proteins. This suggests that most of the identified proteins interact with Bqt4

245 independent of the APSES domain or that its interaction is mediated by other proteins and/or DNA.

246 According to the GO classification, proteins related to nucleocytoplasmic transport (Imp1,
247 Cut15, and Kap95; FE = 5.81) were enriched as Bqt4-binding proteins. Notably, importin β /karyopherin,
248 but not importin α , was identified as a Lem2-binding protein, whereas both importin α and β were
249 identified as Bqt4-binding proteins. This suggests that Bqt4 plays a role in the recruitment of importin α
250 to INM. The 19S proteasome subunits, Rpn1 and Rpt2, were also detected. This is consistent with our
251 previous report that Bqt4 is degraded in the absence of Bqt3 (27), implying that Bqt4 is degraded via a
252 proteasome-dependent pathway.

253 Among the Bqt4-binding proteins, seven proteins (Ape2, Rad25, Bip1, Pfk1, Ura1, Sum3, and
254 Tif35) were shared with Lem2-binding proteins. Rad25 and Rad24, which are 14-3-3 protein homologs in
255 *S. pombe*, were detected (Table 2), suggesting that Bqt4 and Lem2 cooperatively regulate the cell cycle
256 checkpoints at G2/M phase (42). Cwh43, which is involved in triacylglycerol metabolism (43), was found
257 only in the Bqt4-binding proteins. GFP-Cwh43 was localized to the NE (or perinuclear ER) and deletion
258 of *bqt4*⁺ did not affect its localization (Fig. 3D).

259 As Lem2 interacts with a different set of lipid synthesis enzymes than Bqt4, the nuclear
260 membrane ruptures caused by the double deletion of *lem2*⁺ and *bqt4*⁺ genes could be explained by the
261 involvement of different lipid metabolic processes via the interactions of Lem2 and Bqt4 with different
262 lipid synthesis enzymes. Consistently, lipid metabolism has been reported to be important for the
263 maintenance of the inner nuclear membrane in *S. cerevisiae* (44). It has also been reported that the
264 synthesis of glycerophospholipid is required for nuclear membrane expansion, especially during cell
265 division, in fission yeasts (45, 46). Collectively, our results suggest that regulation of lipid synthesis in the
266 NE and ER may be necessary to maintain nuclear functions.

267

268 **Conclusion**

269 In this study, we identified 45 Lem2-binding proteins and 23 Bqt4-binding proteins via IP and MS

270 analysis. Nine proteins identified in Lem2, including Cho2, Ole1, and Erg11, were involved in lipid
271 synthesis. Chw43, which was identified only in Bqt4, was involved in glucosylceramide synthesis. Our
272 results suggest that Lem2 and Bqt4 may regulate different processes of lipid synthesis.

273

274 **Footnotes**275 **Acknowledgments**

276 We thank Chizuru Ohtsuki and Naomi Takagi for their technical assistance. This study was supported by
277 JSPS KAKENHI Grant Numbers JP19K06489 and JP20H05891 (to Y. Hirano), JP19K23725 and
278 JP21K15017 (to Y.K.), JP22H02546, JP22H05599, JP19H03156, JP18H04713, and JP18H05532 (to
279 C.O.), JP18H05528 (to T.H.), and JP18H05533, JP19K22389 and JP20H00454 (to Y. Hiraoka).

280

281 **Author Contributions**

282 Y. Hirano, Y. K., and C. O. carried out the experiments. Y. Hirano, Y. K., T. H. and Y. Hiraoka designed
283 experiments and analyzed the data sets. Y. Hirano, T. H. and Y. Hiraoka prepared the manuscript. C.O., T.
284 H. and Y. Hiraoka supervise the project.

285

286 **Reference**

- 287 1. Harr, J. C., Gonzalez-Sandoval, A., and Gasser, S. M. (2016) Histones and histone modifications
288 in perinuclear chromatin anchoring: from yeast to man. *EMBO Rep* **17**, 139-155
- 289 2. Towbin, B. D., Gonzalez-Sandoval, A., and Gasser, S. M. (2013) Mechanisms of heterochromatin
290 subnuclear localization. *Trends Biochem Sci* **38**, 356-363
- 291 3. Van De Vosse, D. W., Wan, Y., Wozniak, R. W., and Aitchison, J. D. (2011) Role of the nuclear
292 envelope in genome organization and gene expression. *WIREs Syst. Biol. Med.* **3**, 147-166
- 293 4. Padeken, J., Methot, S. P., and Gasser, S. M. (2022) Establishment of H3K9-methylated
294 heterochromatin and its functions in tissue differentiation and maintenance. *Nat. Rev. Mol. Cell*
295 *Biol.* **23**, 623-640
- 296 5. Lim, S., Quinton, R. J., and Ganem, N. J. (2016) Nuclear envelope rupture drives genome instability
297 in cancer. *Mol. Biol. Cell* **27**, 3210-3213
- 298 6. Kinuagsa, Y., Hirano, Y., Sawai, M., Ohno, Y., Shindo, T., Asakawa, H., Chikashige, Y., Shibata,
299 S., Kihara, A., Haraguchi, T., and Hiraoka, Y. (2019) Very-long-chain fatty acid elongase Elo2
300 rescues lethal defects associated with loss of the nuclear barrier function. *J. Cell Sci.* **132**, jcs229021
- 301 7. Webster, B. M., and Lusk, C. P. (2016) Border Safety: Quality Control at the Nuclear Envelope.
302 *Trends in Cell Biol.* **26**, 29-39
- 303 8. Schirmer, E. C., Florens, L., Guan, T., Yates, J. R., and Gerace, L. (2003) Nuclear membrane
304 proteins with potential disease links found by subtractive proteomics. *Science* **301**, 1380-1382
- 305 9. Korfali, N., Wilkie, G. S., Swanson, S. K., Srsen, V., De Las Heras, J., Batrakou, D. G., Malik, P.,
306 Zuleger, N., Kerr, A. R. W., Florens, L., and Schirmer, E. C. (2012) The nuclear envelope proteome
307 differs notably between tissues. *Nucleus* **3**, 552-564
- 308 10. De Las Heras, J. I., Meinke, P., Batrakou, D. G., Srsen, V., Zuleger, N., Kerr, A. R., and Schirmer,
309 E. C. (2013) Tissue specificity in the nuclear envelope supports its functional complexity. *Nucleus*
310 **4**, 460-477

- 311 11. Iwamoto, M., Fukuda, Y., Osakada, H., Mori, C., Hiraoka, Y., and Haraguchi, T. (2019)
312 Identification of the evolutionarily conserved nuclear envelope proteins Lem2 and MicLem2 in
313 *Tetrahymena thermophila*. *Gene X* **1**, 100006
- 314 12. Hiraoka, Y., Maekawa, H., Asakawa, H., Chikashige, Y., Kojidani, T., Osakada, H., Matsuda, A.,
315 and Haraguchi, T. (2011) Inner nuclear membrane protein Imal is dispensable for intranuclear
316 positioning of centromeres. *Genes Cells* **16**, 1000-1011
- 317 13. Mans, B., Anantharaman, V., Aravind, L., and Koonin, E. V. (2004) Comparative Genomics,
318 Evolution and Origins of the Nuclear Envelope and Nuclear Pore Complex. *Cell Cycle* **3**, 1625-
319 1650
- 320 14. Brachner, A., and Foisner, R. (2011) Evolvement of LEM proteins as chromatin tethers at the
321 nuclear periphery. *Biochem. Soc. Trans.* **39**, 1735-1741
- 322 15. Gu, M., LaJoie, D., Chen, O. S., von Appen, A., Ladinsky, M. S., Redd, M. J., Nikolova, L.,
323 Bjorkman, P. J., Sundquist, W. I., Ullman, K. S., and Frost, A. (2017) LEM2 recruits CHMP7 for
324 ESCRT-mediated nuclear envelope closure in fission yeast and human cells. *Proc. Natl. Acad. Sci.*
325 *USA* **114**, E2166-E2175
- 326 16. Von Appen, A., Lajoie, D., Johnson, I. E., Trnka, M. J., Pick, S. M., Burlingame, A. L., Ullman, K.
327 S., and Frost, A. (2020) LEM2 phase separation promotes ESCRT-mediated nuclear envelope
328 reformation. *Nature* **582**, 115-118
- 329 17. Thaller, D. J., Tong, D., Marklew, C. J., Ader, N. R., Mannino, P. J., Borah, S., King, M. C., Ciani,
330 B., and Lusk, C. P. (2021) Direct binding of ESCRT protein Chm7 to phosphatidic acid-rich
331 membranes at nuclear envelope herniations. *J. Cell Biol.* **220**, e202004222
- 332 18. Pieper, G. H., Sprenger, S., Teis, D., and Oliferenko, S. (2020) ESCRT-III/Vps4 Controls
333 Heterochromatin-Nuclear Envelope Attachments. *Dev. Cell* **53**, 27-41.e26
- 334 19. Lee, I.-J., Stokasimov, E., Dempsey, N., Varberg, J. M., Jacob, E., Jaspersen, S. L., and Pellman, D.
335 (2020) Factors promoting nuclear envelope assembly independent of the canonical ESCRT pathway.

336 *J. Cell Biol.* **219**

- 337 20. Barrales, R. R., Forn, M., Georgescu, P. R., Sarkadi, Z., and Braun, S. (2016) Control of
338 heterochromatin localization and silencing by the nuclear membrane protein Lem2. *Genes Dev.* **30**,
339 133-148
- 340 21. Bandy, S., Farooq, Z., Rashid, R., Abdullah, E., and Altaf, M. (2016) Role of Inner Nuclear
341 Membrane Protein Complex Lem2-Nur1 in Heterochromatic Gene Silencing. *J. Biol. Chem.* **291**,
342 20021-20029
- 343 22. Tange, Y., Chikashige, Y., Takahata, S., Kawakami, K., Higashi, M., Mori, C., Kojidani, T., Hirano,
344 Y., Asakawa, H., Murakami, Y., Haraguchi, T., and Hiraoka, Y. (2016) Inner nuclear membrane
345 protein Lem2 augments heterochromatin formation in response to nutritional conditions. *Genes*
346 *Cells* **21**, 812-832
- 347 23. Martín Caballero, L., Capella, M., Barrales, R. R., Dobrev, N., van Emden, T., Hirano, Y., Suma
348 Sreechakram, V. N., Fischer-Burkart, S., Kinugasa, Y., Nevers, A., Rougemaille, M., Sinning, I.,
349 Fischer, T., Hiraoka, Y., and Braun, S. (2022) The inner nuclear membrane protein Lem2
350 coordinates RNA degradation at the nuclear periphery. *Nat. Struct. Mol. Biol.* **29**, 910-921
- 351 24. Hirano, Y., Kinugasa, Y., Osakada, H., Shindo, T., Kubota, Y., Shibata, S., Haraguchi, T., and
352 Hiraoka, Y. (2020) Lem2 and Lnp1 maintain the membrane boundary between the nuclear envelope
353 and endoplasmic reticulum. *Commun. Biol.* **3**, 276
- 354 25. Kume, K., Cantwell, H., Burrell, A., and Nurse, P. (2019) Nuclear membrane protein Lem2
355 regulates nuclear size through membrane flow. *Nat. Commun.* **10**, 1871
- 356 26. Hirano, Y., Kinugasa, Y., Asakawa, H., Chikashige, Y., Obuse, C., Haraguchi, T., and Hiraoka, Y.
357 (2018) Lem2 is retained at the nuclear envelope through its interaction with Bqt4 in fission yeast.
358 *Genes Cells* **23**, 122-135
- 359 27. Chikashige, Y., Yamane, M., Okamasa, K., Tsutsumi, C., Kojidani, T., Sato, M., Haraguchi, T., and
360 Hiraoka, Y. (2009) Membrane proteins Bqt3 and -4 anchor telomeres to the nuclear envelope to

- 361 ensure chromosomal bouquet formation. *J. Cell Biol.* **187**, 413-427
- 362 28. Chikashige, Y., Tsutsumi, C., Yamane, M., Okamasa, K., Haraguchi, T., and Hiraoka, Y. (2006)
- 363 Meiotic proteins bqt1 and bqt2 tether telomeres to form the bouquet arrangement of chromosomes.
- 364 *Cell* **125**, 59-69
- 365 29. Varberg, J. M., Gardner, J. M., Mccroskey, S., Saravanan, S., Bradford, W. D., and Jaspersen, S. L.
- 366 (2020) High-Throughput Identification of Nuclear Envelope Protein Interactions in
- 367 *Schizosaccharomyces pombe* Using an Arrayed Membrane Yeast-Two Hybrid Library. *G3* **10**,
- 368 4649-4663
- 369 30. Moreno, S., Klar, A., and Nurse, P. (1991) Molecular genetic analysis of fission yeast
- 370 *Schizosaccharomyces pombe*. *Methods Enzymol.* **194**, 795-823
- 371 31. Bähler, J., Wu, J. Q., Longtine, M. S., Shah, N. G., McKenzie, A., Steever, A. B., Wach, A.,
- 372 Philippsen, P., and Pringle, J. R. (1998) Heterologous modules for efficient and versatile PCR-
- 373 based gene targeting in *Schizosaccharomyces pombe*. *Yeast* **14**, 943-951
- 374 32. Wach, A. (1996) PCR-synthesis of marker cassettes with long flanking homology regions for gene
- 375 disruptions in *S. cerevisiae*. *Yeast* **12**, 259-265
- 376 33. Nozawa, R. S., Nagao, K., Masuda, H. T., Iwasaki, O., Hirota, T., Nozaki, N., Kimura, H., and
- 377 Obuse, C. (2010) Human POGZ modulates dissociation of HP1alpha from mitotic chromosome
- 378 arms through Aurora B activation. *Nat. Cell Biol.* **12**, 719-727
- 379 34. Asakawa, H., Kojidani, T., Yang, H. J., Ohtsuki, C., Osakada, H., Matsuda, A., Iwamoto, M.,
- 380 Chikashige, Y., Nagao, K., Obuse, C., Hiraoka, Y., and Haraguchi, T. (2019) Asymmetrical
- 381 localization of Nup107-160 subcomplex components within the nuclear pore complex in fission
- 382 yeast. *PLoS Genet.* **15**, e1008061
- 383 35. Harris, M. A., Rutherford, K. M., Hayles, J., Lock, A., Bähler, J., Oliver, S. G., Mata, J., and Wood,
- 384 V. (2022) Fission stories: using PomBase to understand *Schizosaccharomyces pombe* biology.
- 385 *Genetics* **220**, iyab222

- 386 36. Matsuda, A., Chikashige, Y., Ding, D. Q., Ohtsuki, C., Mori, C., Asakawa, H., Kimura, H.,
387 Haraguchi, T., and Hiraoka, Y. (2015) Highly condensed chromatins are formed adjacent to
388 subtelomeric and decondensed silent chromatin in fission yeast. *Nat. Commun.* **6**, 7753
- 389 37. Schindelin, J., Arganda-Carreras, I., Frise, E., Kaynig, V., Longair, M., Pietzsch, T. *et al.* (2012)
390 Fiji: an open-source platform for biological-image analysis *Nat. Methods* **9**, 676-682
- 391 38. Gonzalez, Y., Saito, A., and Sazer, S. (2012) Fission yeast Lem2 and Man1 perform fundamental
392 functions of the animal cell nuclear lamina. *Nucleus* **3**, 60-76
- 393 39. Lucena, R., Dephoure, N., Gygi, S. P., Kellogg, D. R., Tallada, V. A., Daga, R. R., and Jimenez, J.
394 (2015) Nucleocytoplasmic transport in the midzone membrane domain controls yeast mitotic
395 spindle disassembly. *J. Cell Biol.* **209**, 387-402
- 396 40. King, M. C., Lusk, C., and Blobel, G. (2006) Karyopherin-mediated import of integral inner nuclear
397 membrane proteins. *Nature* **442**, 1003-1007
- 398 41. Hu, C., Inoue, H., Sun, W., Takeshita, Y., Huang, Y., Xu, Y., Kanoh, J., and Chen, Y. (2019)
399 Structural insights into chromosome attachment to the nuclear envelope by an inner nuclear
400 membrane protein Bqt4 in fission yeast. *Nucleic Acids Res.* **47**, 1573-1584
- 401 42. Lopez-Girona, A., Furnari, B., Mondesert, O., and Russell, P. (1999) Nuclear localization of Cdc25
402 is regulated by DNA damage and a 14-3-3 protein. *Nature* **397**, 172-175
- 403 43. Nakazawa, N., Teruya, T., Sajiki, K., Kumada, K., Villar-Briones, A., Arakawa, O., Takada, J.,
404 Saitoh, S., and Yanagida, M. (2018) Fission yeast ceramide ts mutants *cwh43* exhibit defects in G0
405 quiescence, nutrient metabolism, and lipid homeostasis. *J. Cell Sci.* **131**, jcs217331
- 406 44. Romanauska, A. and Köhler, A. (2021) Reprogrammed lipid metabolism protects inner nuclear
407 membrane against unsaturated fat. *Dev. Cell* **56**, 2562-2578
- 408 45. Foo, S., Cazenave-Gassiot, A., Wenk, M. R., and Oliferenko, S. (2023) Diacylglycerol at the inner
409 nuclear membrane fuels nuclear envelope expansion in closed mitosis. *J. Cell Sci.* **136**, jcs260568
- 410 46. Takemoto, A., Kawashima, S. A., Li, J. J., Jeffery, L., Yamatsugu, K., Elemento, O. *et al.* (2016)

411 Nuclear envelope expansion is crucial for proper chromosomal segregation during a closed mitosis

412 *J. Cell Sci.* **129**, 1250-1259 10.1242/jcs.181560

413

414 **Figure legends**415 **Figure 1. Identification of Lem2-binding proteins.**

416 (A) Subcellular localization of FLAG-Lem2-HA (right panels) or FLAG-HA (left panels, as a control) in
417 *Schizosaccharomyces pombe* cells. Cells expressing FLAG-Lem2-HA or FLAG-HA were stained via
418 indirect immunofluorescence staining using anti-HA antibody and observed via fluorescence microscopy.
419 Black signals represent high fluorescence signals. Nuclear regions (pink square) are enlarged on the right.
420 Bar: 10 μ m.

421 (B) SDS-PAGE analysis of Lem2-binding proteins obtained via immunoprecipitation (IP). Proteins were
422 stained via silver staining. Molecular weights of the markers are shown on the left of each gel. Left panel:
423 One-step purification of Lem2-binding proteins. Cells expressing FLAG-Lem2-HA (Lem2) or FLAG-HA
424 as a control (Cont) were lysed in the CSK-HEPES buffer containing 150 or 300 mM NaCl. Cell lysates
425 were subjected to IP using anti-HA antibody to obtain Lem2-binding proteins. Loaded samples are
426 indicated at the top of each lane: molecular weight markers (MW), FLAG-HA as a control (Cont), FLAG-
427 Lem2-HA (Lem2), and 20 ng BSA as a loading marker (BSA). Red asterisks indicate the heavy and light
428 chains of the anti-HA antibody. Right panel: Two-step purification of Lem2-binding proteins in the
429 presence or absence of endogenous Lem2. FLAG-Lem2-HA (Lem2) or FLAG-HA (Cont) were expressed
430 in *lem2*⁺ and *lem2* Δ cells. Cells were lysed in CSK-HEPES buffer containing 150 mM NaCl, and cell
431 lysates were subjected to IP using the anti-FLAG antibody and subsequently the anti-HA antibody. MW
432 and BSA are as described above. Numbers at the bottom represent the sample numbers for mass
433 spectrometry analysis.

434 (C) Classification of the 45 proteins identified via mass spectrometry. These proteins were classified
435 according to gene ontology (GO) terms and the results are shown as a pie chart. The value in parentheses
436 represents fold enrichment of the GO term.

437

438 Figure 2. Characterization of Lem2-binding proteins Cho2, Ole1, and Erg11.

439 (A) Western blotting of GFP-Cho2 (left panels), GFP-Ole1 (middle panels), and Erg11-GFP (right
440 panels). A GFP-fused protein (GFP-Cho2, GFP-Ole1, or Erg11-GFP) was expressed in *S. pombe* wild-
441 type (WT) expressing FLAG-Lem2-HA and *bqt4* Δ cells expressing FLAG-Lem2-HA. Cell lysates were
442 subjected to IP using anti-FLAG antibody beads, and the bound GFP-tagged proteins were detected using
443 anti-GFP or anti-HA antibodies. GFP was used as a control for GFP-fused proteins. For Cho2 IP, 0.5 and
444 0.01% input were loaded for GFP and GFP-Cho2, respectively. For Ole1 and Erg11 IP, 0.2% input was
445 loaded. Molecular weight markers (MW) are shown on the left. Asterisks indicate the non-specific bands.
446 (B) Subcellular localization of GFP-Cho2, GFP-Ole1, and Erg11-GFP. One of the GFP-fused proteins was
447 expressed in *S. pombe* WT or *lem2* Δ cells and its localization was observed via fluorescence microscopy.
448 Black signals represent high fluorescence signals. Due to the different expression levels of these proteins,
449 the display scale of the images was adjusted individually: among these three proteins, Cho2 was the
450 highest and Erg11 the lowest in the expression level. Bar: 5 μ m.

451

452 Figure 3. Identification and characterization of Bqt4-binding proteins.

453 (A) SDS-PAGE of Bqt4-binding proteins obtained via IP. Cells expressing FLAG-Bqt4-HA or FLAG-HA
454 were lysed in the CSK-HEPES buffer containing 150 mM NaCl. Binding proteins were obtained via two-
455 step purification using the anti-FLAG antibody and subsequently the anti-HA antibody. Purified proteins
456 were subjected to SDS-PAGE and detected via silver staining.
457 Loaded samples are indicated at the top of each lane: molecular weight markers (MW), FLAG-HA as a
458 control (Cont), FLAG-Bqt4-HA (Bqt4), and 20 ng BSA as a loading marker (BSA). Molecular weights of
459 the markers are shown on the left side.

460 (B) Classification of the 23 identified proteins. These proteins were classified according to GO terms and
461 the results are shown as a pie chart. The value in parentheses represents the fold enrichment of the GO
462 term.

463 (C) Western blotting of GFP-Bqt3 (left) and GFP-Lem2 (right). GFP-Bqt3 or Lem2-GFP was expressed in
464 *S. pombe* cells expressing FLAG-Bqt4-HA. GFP-expressing cells were used as controls for GFP-Bqt3 and
465 Lem2-GFP. After IP with an anti-FLAG antibody, bound GFP-tagged proteins were detected using anti-
466 GFP or anti-HA antibodies. The number of proteins loaded into the input was 0.5%. Samples were loaded
467 as indicated on the top of each lane: GFP as a control (Cont); GFP-Bqt3 (Bqt3); Lem2-GFP (Lem2).

468 Molecular weight markers are shown on the left. Asterisks indicate the non-specific bands.

469 (D) Subcellular localization of GFP-Cwh43. GFP-Cwh43 was expressed in *S. pombe* WT or *bq4Δ* cells
470 and its localization was observed via fluorescence microscopy. Black signals represent high fluorescence
471 signals. Bar: 5 μ m.

472

473 **Conflict of interest**

474 The authors declare that they have no conflicts of interest with the contents of this article.

Table 1. Lem2-binding proteins. The proteins shown in Fig.1B were identified by LC/MS. Numbers indicate the number of detected peptides by LC/MS analysis. GO classification shown here is based on PomBase.

Name	Identified Proteins Description	Accession Number	MW (kDa)	Trans- membrane domain	<i>lem2</i> ⁺						<i>lem2</i> Δ		GO slim	GO	Ref.		
					One-step purification (HA)				Two-step purification (FLAG→HA)							control	lem2
					150mM NaCl		300mM NaCl		150mM NaCl		control	lem2					
					control	lem2	control	lem2	control	lem2						control	lem2
Lem2	LEM domain nuclear inner membrane protein Heh1/Lem2	SPAC18G6.10	78	2	0	89	0	48	0	283	2	287					
Bqt4	bouquet formation protein Bqt4	SPBC19C7.10	48	1	0	10	0	7	0	14	0	15	telomere organization	telomere organization	Hirano Y et al. (2018)		
Cho2	phosphatidylethanolamine N-methyltransferase Cho2	SPBC26H8.03	103	10	0	18	0	4	0	19	0	16	lipid metabolic process	phosphatidylcholine biosynthetic process	Varberg JM et al. (2020)		
Ole1	acyl-coA desaturase	SPCC1281.06c	54	3	0	9	0	1	0	15	0	19	lipid metabolic process	unsaturated fatty acid biosynthetic process			
Nmd5	karyopherin/importin beta family nuclear import/export signal receptor	SPCC550.11	116	0	0	8	0	1	0	8	0	10	nucleocytoplasmic transport	protein import into nucleus			
Erg11	sterol 14-demethylase	SPAC13A11.02c	56	2	0	5	0	1	0	3	0	2	lipid metabolic process	ergosterol biosynthetic process			
Ape2	aminopeptidase Ape2	SPBC1921.05	99	0	0	4	0	1	0	8	0	8	protein targeting	cytoplasm to vacuole transport by the NVT pathway			
Rad25	14-3-3 protein Rad25	SPAC17A2.13c	30	0	0	4	0	1	0	7	0	9	mitotic cell cycle phase transition	mitotic G2 DNA damage checkpoint signaling			
Rpl6	60S ribosomal protein L6	SPCC622.18	21	0	0	3	0	1	0	3	0	7	cytoplasmic translation	cytoplasmic translation			
Pfk1	6-phosphofructokinase	SPBC16H5.02	103	0	0	22	0	0	0	7	0	6	carbohydrate metabolic process	glycolytic process			
Hmg1	3-hydroxy-3-methylglutaryl-CoA reductase Hmg1	SPCC162.09c	115	7	0	15	0	0	0	12	0	13	lipid metabolic process	ergosterol biosynthetic process			
Rpl402	60S ribosomal protein L2	SPBP8B7.03c	40	0	0	14	0	0	0	7	0	9	cytoplasmic translation	cytoplasmic translation			
Met10	sulfite reductase NADPH flavoprotein subunit	SPCC584.01c	111	0	0	12	0	0	0	5	0	6	sulfur compound metabolic process	hydrogen sulfide biosynthetic process			
Ura1	carbamoyl-phosphate synthase	SPAC22G7.06c	248	0	0	12	0	0	0	17	0	20	amino acid metabolic process	de novo' pyrimidine nucleobase biosynthetic process			
Gcn1	translation initiation regulator, HEAT repeat protein Gcn1	SPAC18G6.05c	297	0	0	11	0	0	0	11	0	10	cytoplasmic translation	cellular response to amino acid starvation			
Sum3	ATP-dependent RNA helicase Sum3	SPCC1795.11	70	0	0	8	0	0	0	3	0	2	cytoplasmic translation	cytoplasmic translational initiation			
Fas1	fatty acid synthase beta subunit Fas1	SPAC926.09c	231	0	0	8	0	0	0	5	0	4	lipid metabolic process	fatty acid biosynthetic process			
Rpl13	60S ribosomal protein L13	SPAC664.05	24	0	0	8	0	0	0	3	0	4	cytoplasmic translation	cytoplasmic translation			
Bfr1	brefeldin A efflux transporter Bfr1	SPCC18B5.01c	172	12	0	7	0	0	0	7	0	15	transmembrane transport	xenobiotic detoxification by transmembrane export across the plasma membrane			
Wbp1	dolichyl-di-phosphooligosaccharide-protein glycotransferase subunit Wbp1	SPCC338.15	49	1	0	7	0	0	0	6	0	8	protein glycosylation	protein N-linked glycosylation via asparagine			
SPAC11D3.14c	5-oxoprolinase (ATP-hydrolyzing)	SPAC11D3.14c	139	0	0	6	0	0	0	13	0	10	sulfur compound metabolic process	cellular detoxification			
SPBC1703.13c	mitochondrial inorganic phosphate transporter	SPBC1703.13c	34	3	0	5	0	0	0	4	0	12	transmembrane transport	mitochondrial transport			

Lys4	homocitrate synthase	SPBC1105.02c	46	0	0	5	0	0	0	7	0	12	amino acid metabolic process	lysine biosynthetic process
Rpl701	60S ribosomal protein L7	SPBC18H10.12c	29	0	0	5	0	0	0	5	0	6	tRNA metabolic process	endonucleolytic cleavage involved in tRNA processing
Bip1	ER heat shock protein BiP	SPAC22A12.15c	73	1	0	4	0	0	0	25	0	14	protein catabolic process	ubiquitin-dependent ERAD pathway
Erg5	C-22 sterol desaturase Erg5	SPAC19A8.04	62	0	0	4	0	0	0	6	0	6	lipid metabolic process	ergosterol biosynthetic process
Rpp0	60S acidic ribosomal protein Rpp0	SPCC18.14c	34	0	0	4	0	0	0	3	0	3	cytoplasmic translation	cytoplasmic translational elongation
Atp1	F1-ATPase alpha subunit	SPAC14C4.14	59	0	0	4	0	0	0	6	0	2	transmembrane transport	proton motive force-driven mitochondrial ATP synthesis
Tsc13	enoyl-[acyl-carrier-protein] reductase	SPBC646.07c	35	5	0	4	0	0	0	2	0	4	lipid metabolic process	very long-chain fatty acid biosynthetic process
Cct3	chaperonin-containing T-complex gamma subunit Cct3	SPBC1A4.08c	58	0	0	3	0	0	0	7	0	5	protein folding	protein folding
Tif35	translation initiation factor eIF3g	SPBC18H10.03	31	0	0	3	0	0	0	2	0	4	cytoplasmic translation	formation of cytoplasmic translation initiation complex
Kap123	karyopherin Kap123	SPBC14F5.03c	118	0	0	3	0	0	0	2	0	2	nucleocytoplasmic transport	protein import into nucleus
Pho84	inorganic phosphate transporter	SPBC8E4.01c	64	11	0	2	0	0	0	9	0	7	transmembrane transport	phosphate ion transmembrane transport
Rpl8	60S ribosomal protein L7a/L8	SPBC29A3.04	29	0	0	2	0	0	0	3	0	7	cytoplasmic translation	cytoplasmic translation
Hsp90	Hsp90 chaperone	SPAC926.04c	81	0	0	2	0	0	0	7	0	3	protein folding	protein folding
Lcf1	long-chain-fatty-acid-CoA ligase Lcf1	SPBC18H10.02	76	0	0	2	0	0	0	2	0	3	lipid metabolic process	long-chain fatty acid metabolic process
Adh1	alcohol dehydrogenase Adh1	SPCC13B11.01	37	0	0	2	0	0	0	5	0	3	generation of precursor metabolites and energy	glycolytic fermentation to ethanol
SPBC2G5.01	ER membrane chaperone for multipass membrane proteins, PAT complex subunit, and TMC01 translocon subunit (human CCDC47 ortholog)	SPBC2G5.01	43	1	0	2	0	0	0	3	0	3	membrane organization	protein insertion into ER membrane
Its8	pig-N	SPBC839.08c	106	14	0	2	0	0	0	3	0	2	lipid metabolic process	GPI anchor biosynthetic process
SPBC17A3.05c	DNAJ/DUF1977, human DNAJB12 homolog, Hsp70 co-chaperone	SPBC17A3.05c	46	1	0	2	0	0	0	5	0	4	protein folding	cellular response to misfolded protein
Vtc4	vacuolar transporter chaperone	SPCC1322.14c	84	3	0	2	0	0	0	3	0	2	autophagy	vacuolar transport
Sal3	karyopherin/importin beta family nuclear import signal receptor Sal3	SPCC1840.03	122	0	0	2	0	0	0	12	0	4	nucleocytoplasmic transport	protein import into nucleus
Cka1	serine/threonine protein kinase Cka1	SPAC23C11.11	40	0	0	1	0	0	0	7	0	7	regulation of DNA-templated transcription	cellular response to DNA damage stimulus
Rps101	40S ribosomal protein S3a	SPAC13G6.02c	28	0	0	1	0	0	0	4	0	3	cytoplasmic translation	cytoplasmic translation
Stt3	oligosaccharyltransferase subunit Stt3	SPBC1271.02	85	11	0	1	0	0	0	2	0	3	protein glycosylation	protein N-linked glycosylation
Ost1	dolichyl-diphospho-oligosaccharide-protein glycosyltransferase Ost1	SPAC27F1.07	52	1	0	1	0	0	0	3	0	2	protein glycosylation	protein N-linked glycosylation via asparagine

Table 2. Bqt4-binding proteins. The proteins shown in Fig.3A were identified by LC/MS. Numbers indicate the number of detected peptides by LC/MS analysis. GO classification shown here is based on PomBase.

Identified Proteins		Accession Number	MW (kDa)	Trans-membrane domain	Replicate 1		Replicate 2		GO slim	GO	Ref.
Name	Description				control	Bqt4	control	Bqt4			
Bqt4	bouquet formation protein Bqt4	SPBC19C7.10	48	1	0	172	0	302			
Imp1	importin alpha family nuclear import signal receptor adaptor Imp1	SPBC1604.08c	60	0	0	35	0	84	nucleocytoplasmic transport	protein import into nucleus	Lucena R et al. (2015)
Tef102	Translation elongation factor EF-1 alpha Efl1a-b	SPAC23A1.10	50	0	0	13	0	16	cytoplasmic translation	cytoplasmic translational elongation	
Cut15	importin alpha family nuclear import signal receptor adaptor Cut15	SPCC962.03c	60	0	0	12	0	31	nucleocytoplasmic transport	protein import into nucleus	
Tef3	translation elongation factor eEF3	SPCC417.08	116	0	0	12	0	6	cytoplasmic translation	cytoplasmic translational elongation	
Pma1	plasma membrane P-type proton exporting ATPase, P3-type Pma1	SPAC1071.10c	100	9	0	11	0	35	transmembrane transport	regulation of intracellular pH	
Rad25	14-3-3 protein Rad25	SPAC17A2.13c	30	0	0	7	0	6	mitotic cell cycle phase transition	mitotic G2 DNA damage checkpoint signaling	
Mts4	19S proteasome regulatory subunit Rpn1/Mts4	SPBP19A11.03c	98	0	0	6	0	8	mitotic sister chromatid segregation	proteasomal protein catabolic process	
Pdc101	pyruvate decarboxylase	SPAC1F8.07c	62	0	0	5	0	16	generation of precursor metabolites and energy	generation of precursor metabolites and energy	
Pfk1	6-phosphofructokinase pfk1	SPBC16H5.02	103	0	0	5	0	6	generation of precursor metabolites and energy	glycolytic process	
Ura1	carbamoyl-phosphate synthase	SPAC22G7.06c	248	0	0	4	0	37	amino acid metabolic process	de novo' pyrimidine nucleobase biosynthetic process	
Vid27	WD repeat protein, Vid27 family, conserved in fungi and plants	SPBC1685.14c	92	0	0	4	0	9	Not classified	Not classified	
Rad24	14-3-3 protein Rad24	SPAC8E11.02c	30	0	0	4	0	6	mitotic cell cycle phase transition	mitotic G2 DNA damage checkpoint signaling	
Bip1	ER heat shock protein BiP	SPAC22A12.15c	73	1	0	4	0	5	protein catabolic process	ubiquitin-dependent ERAD pathway	
Ape2	aminopeptidase Ape2	SPBC1921.05	99	0	0	3	0	13	protein targeting	cytoplasm to vacuole transport by the NVT pathway	
Sks2	heat shock protein, Hsp70 family, ribosome associated Sks2	SPBC1709.05	67	0	0	3	0	11	protein folding	ribosome biogenesis	
Kap95	karyopherin/importin beta family nuclear import signal receptor Kap95	SPAC1B1.03c	95	0	0	3	0	9	nucleocytoplasmic transport	protein import into nucleus	
Sec26	coatamer beta subunit	SPBC146.14c	104	0	0	3	0	6	vesicle-mediated transport	intracellular protein transport	
Eft2	translation elongation factor 2 (EF-2) Eft2,A	SPAC513.01c	93	0	0	3	0	3	cytoplasmic translation	cytoplasmic translational elongation	
Rpt2	19S proteasome base subcomplex ATPase subunit Rpt2	SPBC4.07c	50	0	0	3	0	2	mitotic sister chromatid segregation	proteasomal protein catabolic process	
Sum3	translation initiation RNA helicase Sum3	SPCC1795.11	70	0	0	2	0	4	cytoplasmic translation	cytoplasmic translational elongation	
Tif35	translation initiation factor eIF3g	SPBC18H10.03	31	0	0	2	0	3	cytoplasmic translation	formation of cytoplasmic translation initiation complex	
Cwh43	glycosylceramide biosynthesis protein Cwh43	SPAC589.12	110	19	0	2	0	2	lipid metabolic process	GPI anchor biosynthetic process	
Alg9	mannosyltransferase complex subunit Alg9	SPAC1834.05	66	10	0	2	0	2	lipid metabolic process	dolichol-linked oligosaccharide biosynthetic process	

Figure 1

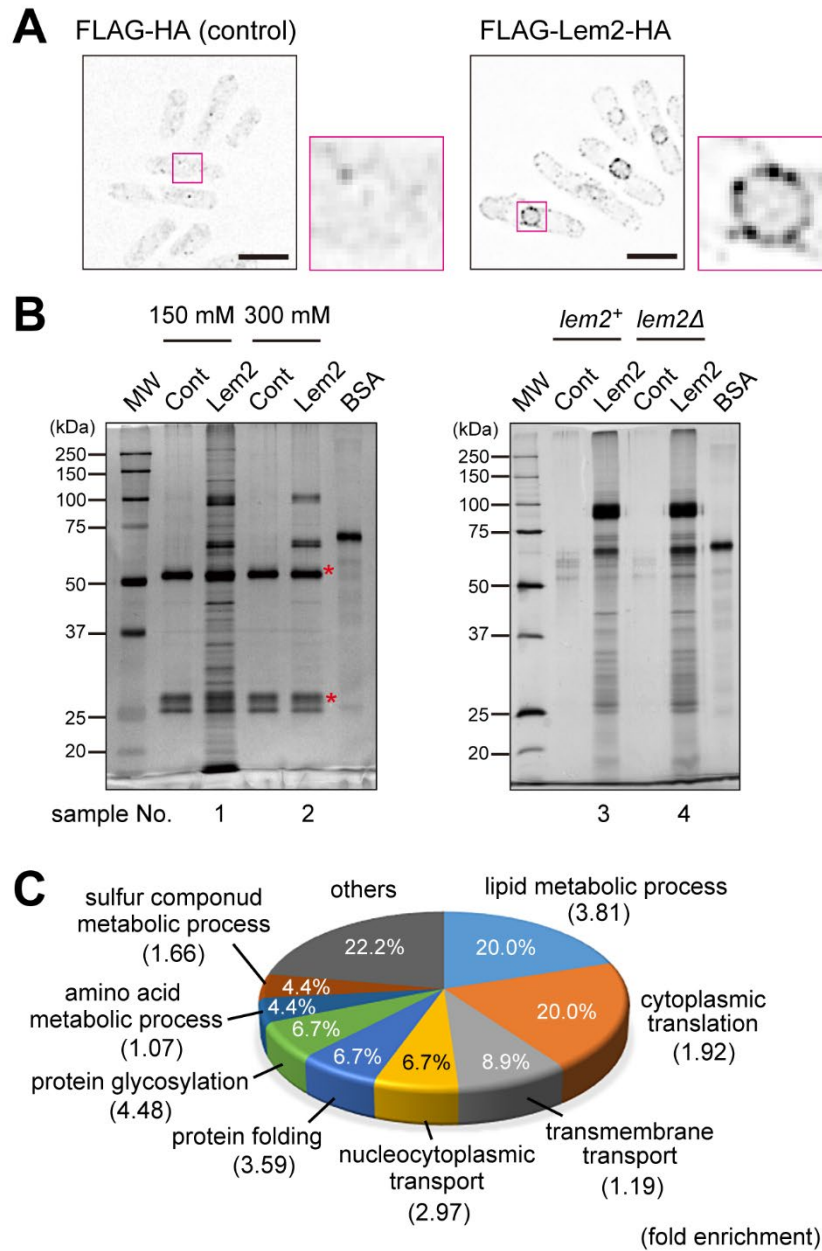


Figure 2

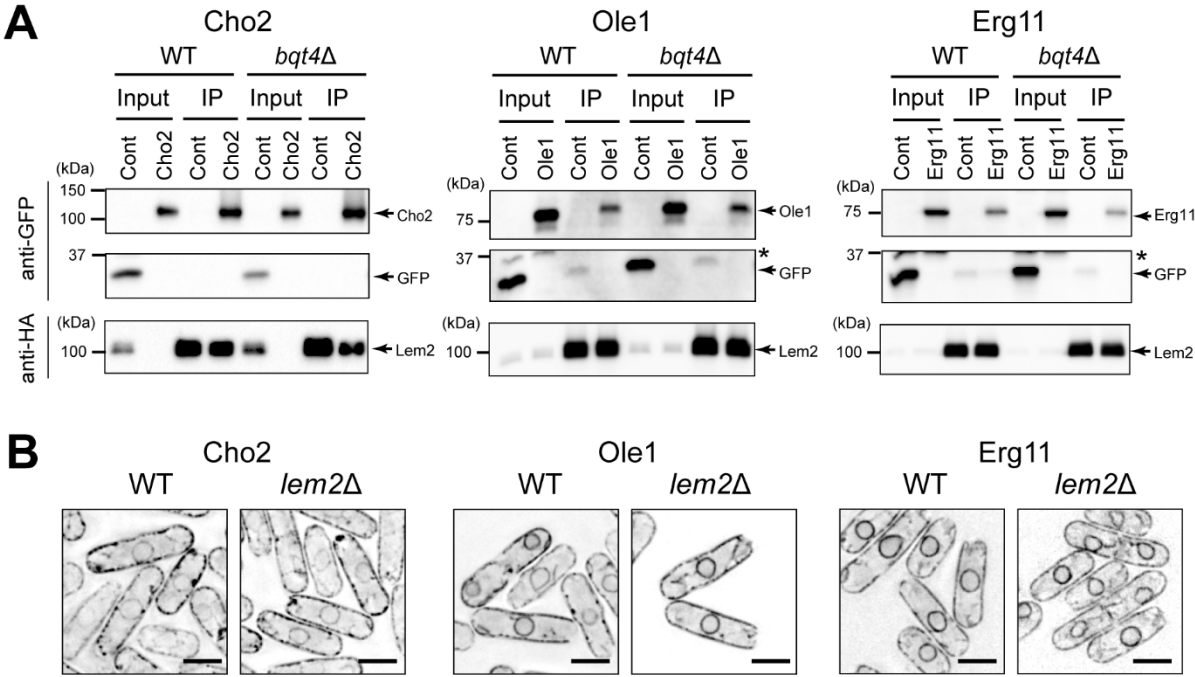
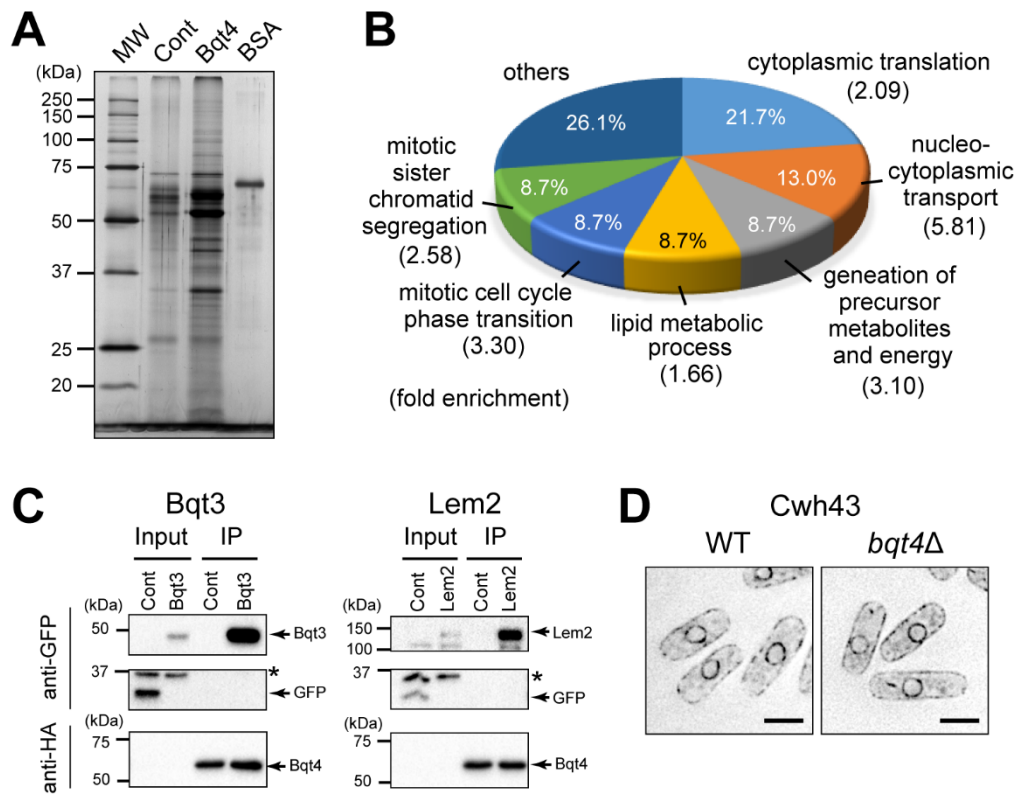
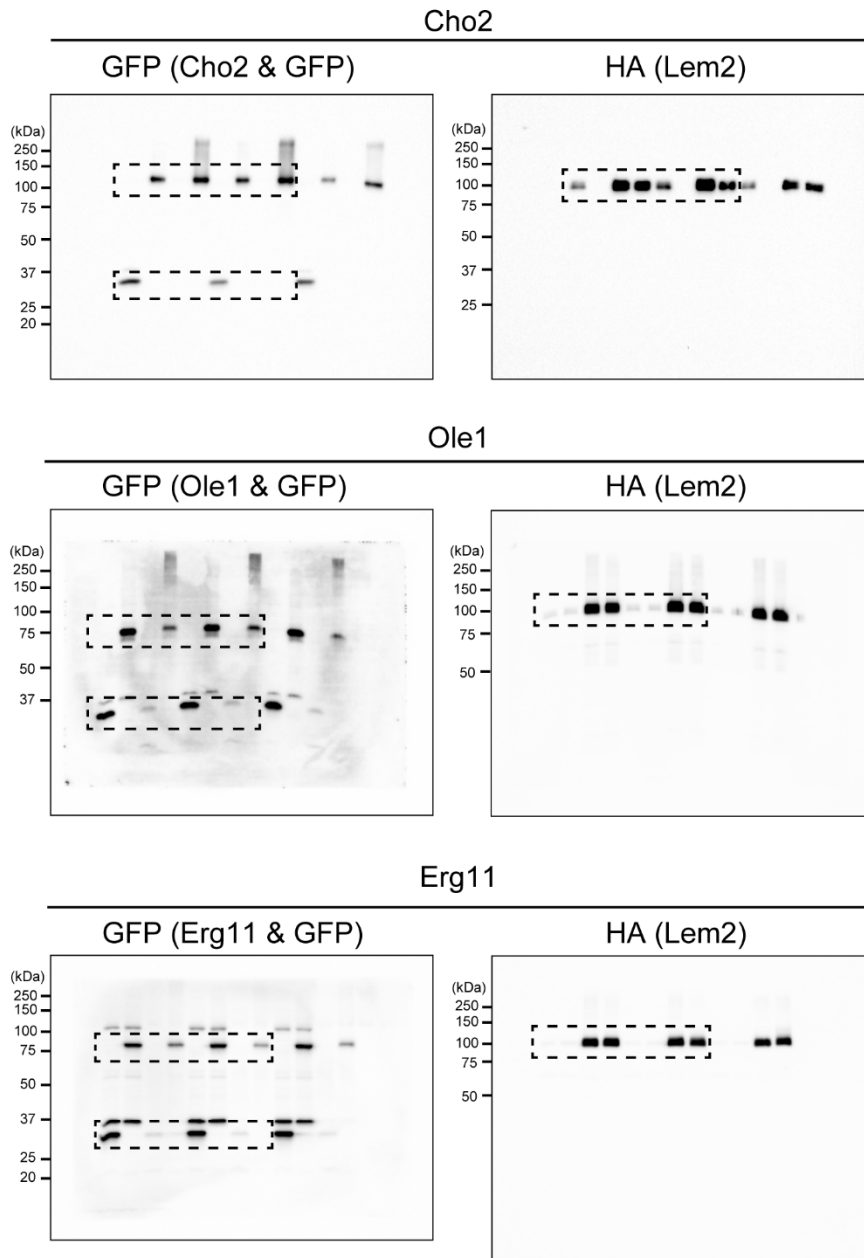


Figure 3

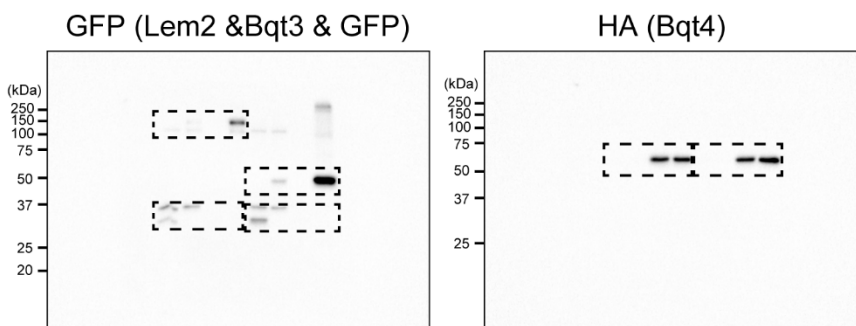


Supplementary Data 1

Full blot for Figure 2A



Full blot for Figure 3C



Supplementary Table 1. *S. pombe* strains used in this study

Strain	Genotype	Source	Figure
H1N1	<i>h⁻ lys1⁺::nmt1p-FLAG-HA</i>	This study	1A-C
H1N3	<i>h⁻ lys1⁺::nmt1p-FLAG-lem2-HA</i>	This study	1 A-C
YK214	<i>h⁻ lys1⁺::nmt1p-FLAG-HA lem2Δ::kan^r</i>	This study	1C
YK215	<i>h⁻ lys1⁺::nmt1p-FLAG-lem2-HA lem2Δ::kan^r</i>	This study	1C
H1N1082	<i>h⁻ lys1⁺::lem2p-FLAG-lem2-HA lem2Δ::kan^r aur1^r::adh1p-GFP</i>	This study	2A
H1N400	<i>h⁻ lys1⁺::lem2p-FLAG-lem2-HA lem2Δ::hph GFP-cho2⁺::kan^r</i>	This study	2A
H1N1132	<i>h⁻ lys1⁺::lem2p-FLAG-lem2-HA lem2Δ::kan^r aur1^r::adh1p-GFP bqt4Δ::hph</i>	This study	2A
H1N914	<i>h⁻ lys1⁺::lem2p-FLAG-lem2-HA lem2Δ::hph GFP-cho2⁺::kan^r bqt4Δ::NAT</i>	This study	2A
H1N1083	<i>h⁻ lys1⁺::lem2p-FLAG-lem2-HA lem2Δ::hph aur1^r::adh1p-GFP</i>	This study	2A
H1N305	<i>h⁻ lys1⁺::lem2p-FLAG-lem2-HA lem2Δ::hph GFP-ole1⁺::kan^r</i>	This study	2A
H1N1248	<i>h⁻ lys1⁺::lem2p-FLAG-lem2-HA lem2Δ::hph aur1^r::adh1p-GFP bqt4Δ::hph</i>	This study	2A
H1N915	<i>h⁻ lys1⁺::lem2p-FLAG-lem2-HA lem2Δ::hph GFP-ole1⁺::kan^r bqt4Δ::NAT</i>	This study	2A
H1N1084	<i>h⁻ lys1⁺::lem2p-FLAG-lem2-HA lem2Δ::hph aur1^r::adh13p-GFP</i>	This study	2A
H1N984	<i>h⁻ lys1⁺::lem2p-FLAG-lem2-HA lem2Δ::kan^r erg11⁺-GFP::NAT</i>	This study	2A
H1N1186	<i>h⁻ lys1⁺::lem2p-FLAG-lem2-HA lem2Δ::hph aur1^r::adh13p-GFP</i>	This study	2A
H1N968	<i>h⁻ lys1⁺::lem2p-FLAG-lem2-HA lem2Δ::hph erg11⁺-GFP::kan^r bqt4Δ::hph</i>	This study	2A
H1N927	<i>h⁺ Ish1⁺-mCherry::bsd GFP-cho2⁺::NAT</i>	This study	2B
H1N928	<i>h⁺ Ish1⁺-mCherry::bsd GFP-cho2⁺::NAT lem2Δ::kan^r</i>	This study	2B
H1N931	<i>h⁺ Ish1⁺-mCherry::bsd GFP-ole1⁺::NAT</i>	This study	2B
H1N932	<i>h⁺ Ish1⁺-mCherry::bsd GFP-ole1⁺::NAT lem2Δ::kan^r</i>	This study	2B
H1N963	<i>h⁺ Ish1⁺-mCherry::bsd erg11⁺-GFP ::NAT</i>	This study	2B
H1N964	<i>h⁺ Ish1⁺-mCherry::bsd erg11⁺-GFP ::NAT lem2Δ::kan^r</i>	This study	2B
H1N165	<i>h⁻ lys1⁺::nmt41p-FLAG-HA</i>	This study	3A
H1N123	<i>h⁻ lys1⁺::nmt41p-FLAG-bqt4-HA</i>	This study	3A
H1N2729	<i>h⁻ lys1⁺::nmt41p-FLAG-bqt4-HA aur1^r::adh31p-GFP</i>	This study	3B
H1N2730	<i>h⁻ lys1⁺::nmt41p-FLAG-bqt4-HA lem2⁺-GFP::NAT</i>	This study	3B
H1N2727	<i>h⁻ lys1⁺::nmt41p-FLAG-bqt4-HA aur1^r::adh15p-GFP</i>	This study	3B
H1N213	<i>h⁻ lys1⁺::nmt41p-FLAG-bqt4-HA aur1^r::bqt3p-GFP-bqt3</i>	This study	3B
H1N2732	<i>h⁺ lys1⁺-pYC36 ish1⁺-mCherry::bsd cwh43⁺-GFP::NAT</i>	This study	3B
H1N2734	<i>h⁺ bqt4Δ::hph lys1⁺::pYC36 ish1⁺-mCherry::bsd cwh43⁺-GFP::NAT</i>	This study	3B

Supplementary Table S2. Minor Bqt4-binding proteins.

The proteins identified only in one replicate are shown. Numbers indicate the number of detected peptides by LC/MS analysis. Yellow-highlighted are shared proteins with Lem2-binding proteins.

Identified Proteins		Accession Number	MW (kDa)	trans-membrane domain	Replicate 1		Replicate 2	
Name	description				control	Bqt4	control	Bqt4
Gcn1	translation initiation regulator, HEAT repeat protein Gcn1	SPAC18G6.05c	297	0	0	0	0	14
Hmg1	3-hydroxy-3-methylglutaryl-CoA reductase Hmg1	SPCC162.09c	115	7	0	0	0	10
Cho2	phosphatidylethanolamine N-methyltransferase Cho2	SPBC26H8.03	103	10	0	0	0	10
Rpl8	60S ribosomal protein L7a/L8	SPBC29A3.04	29	0	0	0	0	9
Rpl402	60S ribosomal protein L4	SPBP8B7.03c	40	0	0	0	0	9
Bgs4	1,3-beta-glucan synthase subunit Bgs4	SPCC1840.02c	225	16	0	0	0	8
Rar1	cytoplasmic methionine-tRNA ligase Mrs1	SPBC17A3.04c	89	0	0	0	0	8
Erg5	C-22 sterol desaturase Erg5	SPAC19A8.04	62	0	0	0	0	8
Rpl701	60S ribosomal protein L7	SPBC18H10.12c	29	0	0	0	0	8
SPAC22E12.18	human CCNDBP1 ortholog	SPAC22E12.18	38	0	0	0	0	8
Rpt3	19S proteasome base subcomplex ATPase subunit Rpt3	SPCC576.10c	44	0	0	0	0	8
Pho84	plasma membrane inorganic phosphate transmembrane transporter	SPBC8E4.01c	64	11	0	0	0	7
SPBC13E7.07	Schizosaccharomyces specific protein	SPBC13E7.07	31	1	0	0	0	7
Cut6	acetyl-CoA/biotin carboxylase	SPAC56E4.04c	257	0	0	0	0	7
Nup124	nucleoporin Nup124	SPAC30D11.04c	124	0	0	0	0	7
Anc1	mitochondrial carrier, ATP:ADP antiporter Anc1	SPBC530.10c	35	3	0	0	0	6
Ptr1	HECT-type ubiquitin ligase E3 Ptr1	SPAC19D5.04	365	0	0	0	0	6
Bfr1	plasma membrane brefeldin A efflux transporter Bfr1	SPCC18B5.01c	172	12	0	0	0	6
Ght8	plasma membrane hexose:proton symporter, unknown specificity Ght8	SPCC548.06c	60	10	0	0	0	6
Abc2	vacuolar phytochelatin and glutathione S-conjugate ABC family transmembrane transporter Abc2	SPAC3F10.11c	167	14	0	0	0	5
SPBC2G5.01	ER membrane chaperone for multipass membrane proteins, PAT complex subunit, and TMCO1 translocon subunit (human CCDC47 ortholog)	SPBC2G5.01	43	1	0	0	0	5
SPBC1703.13c	mitochondrial carrier, inorganic phosphate/copper	SPBC1703.13c	34	3	0	0	0	5
Nmd5	Nmd5	SPCC550.11	116	0	0	0	0	5
Erm1	ER metallopeptidase Erm1	SPCC1259.02c	92	6	0	0	0	5

Met26	homocysteine methyltransferase Met26	SPAC9.09	85	0	0	0	0	5
Rpl1701	60S ribosomal protein L17	SPBC2F12.04	21	0	0	0	0	4
Bgs3	cell wall 1,3-beta-glucan synthase catalytic subunit Bgs3	SPAC19B12.03	211	16	0	0	0	4
Lcf1	long-chain-fatty-acid-CoA ligase Lcf1	SPBC18H10.02	76	0	0	0	0	4
Sec72	Arf GEF Sec72	SPAC30.01c	207	0	0	0	0	4
Ogm4	ER membrane protein O-mannosyltransferase Ogm4	SPBC16C6.09	90	11	0	0	0	4
Hsp90	Hsp90 chaperone	SPAC926.04c	81	0	0	0	0	4
Zwf1	glucose-6-phosphate 1-dehydrogenase Zwf1	SPAC3A12.18	57	0	0	0	0	4
Ole1	acyl-coA desaturase	SPCC1281.06c	54	3	0	0	0	4
Rpl13	60S ribosomal protein L13	SPAC664.05	24	0	0	0	0	4
SPBC16H5.08c	ribosome biogenesis ATPase, Arb family ABCF2-like	SPBC16H5.08c	69	0	0	0	0	4
Rpl35	60S ribosomal protein L35	SPCC613.05c	14	0	0	0	0	4
Hmt1	vacuolar phytochelatin and glutathione S-conjugate ABC family transmembrane transporter Hmt1	SPCC737.09c	94	10	0	0	0	4
Sec62	ER protein translocation subcomplex subunit Sec62	SPAC17G6.09	32	2	0	0	0	4
SPBC17A3.05c	DNAJ/DUF1977, human DNAJB12 homolog, Hsp70 co-chaperone	SPBC17A3.05c	46	1	0	0	0	4
Rpl2001	60S ribosomal protein L20A	SPAC3A12.10	21	0	0	0	0	4
Rpn11	19S proteasome regulatory subunit, ubiquitin-specific protease subunit Rpn11	SPAC31G5.13	35	0	0	0	0	4
Vps1302	intermembrane lipid transfer protein, chorein family Vps1302	SPBC16C6.02c	339	0	0	0	0	3
SPBC460.01c	amino acid transmembrane transporter	SPBC460.01c	63	11	0	0	0	3
Tsc13	enoyl-[acyl-carrier-protein] reductase	SPBC646.07c	35	5	0	0	0	3
Sir1	sulfite reductase beta subunit Sir1	SPAC10F6.01c	164	0	0	0	0	3
Rpl2301	60S ribosomal protein L23	SPAC3G9.03	15	0	0	0	0	3
SPCC1672.11c	P-type ATPase P5 type	SPCC1672.11c	149	10	0	0	0	3
Lys4	homocitrate synthase	SPBC1105.02c	46	0	0	0	0	3
Cct3	chaperonin-containing T-complex gamma subunit Cct3	SPBC1A4.08c	58	0	0	0	0	3
Rpl301	60S ribosomal protein L3	SPAC17A5.03	44	0	0	0	0	3
Cta4	P-type ATPase family V, transmembrane protein dislocase/calcium transporting ATPase Cta4	SPACUNK4.07c	136	8	0	0	0	3
Rpt6	19S proteasome base subcomplex ATPase subunit Rpt6	SPBC23G7.12c	45	0	0	0	0	3
Mnn9	Golgi mannan polymerase I complex subunit Mnn9	SPAC4F10.10c	38	1	0	0	0	3
Rpl2401	60S ribosomal protein L24	SPAC6G9.09c	17	1	0	0	0	3

Elo1	fatty acid elongase Elo1	SPAC1639.01c	42	7	0	0	0	3
Arg11	N-acetyl-gamma-glutamyl-phosphate reductase/acetylglutamate kinase	SPAC4G9.09c	98	0	0	0	0	3
Phb1	prohibitin Phb1	SPAC1782.06c	31	0	0	0	0	3
Rpl3602	60S ribosomal protein L36	SPBC405.07	11	0	0	0	0	3
Glt1	glutamate synthase (GOGAT) Glt1	SPAPB1E7.07	233	0	0	0	0	2
Rpl6	60S ribosomal protein L6	SPCC622.18	21	0	0	0	0	2
Sam1	S-adenosylmethionine synthetase	SPBC14F5.05c	42	0	0	0	0	2
Ubi3	ribosomal-ubiquitin fusion protein Ubi3	SPAC6G10.11c	17	0	0	0	0	2
Rpl801	60S ribosomal protein L8/L2	SPAC1F7.13c	27	0	0	0	0	2
SPAC11D3.14c	5-oxoprolinase (ATP-hydrolyzing)	SPAC11D3.14c	139	0	0	0	0	2
Cdc48	cdc48, AAA family ATPase involved in ubiquitin-mediated protein degradation Cdc48	SPAC1565.08	90	0	0	0	0	2
Drs1	cytoplasmic aspartate-tRNA ligase Drs1	SPCC1223.07c	67	0	0	0	0	2
Fsf1	mitochondrial carrier, serine Fsf1	SPAC17G6.15c	35	5	0	0	0	2
Nde2	external mitochondrial NADH dehydrogenase (ubiquinone) Nde1/Nde2	SPAC3A11.07	62	0	0	0	0	2
Los1	karyopherin/importin-beta family nuclear import receptor Los1	SPBP8B7.09c	110	0	0	0	0	2
Tlc4	TLC domain-containing protein Tlc4	SPAC17A2.02c	33	7	0	0	0	2
Rpn9	19S proteasome regulatory subunit Rpn9	SPAC607.05	43	0	0	0	0	2
Stt3	oligosaccharyltransferase subunit Stt3	SPBC1271.02	85	11	0	0	0	2
Atp2	F1-FO ATP synthase beta subunit Atp2	SPAC222.12c	57	0	0	0	0	2
Its8	pig-N	SPBC839.08c	106	14	0	0	0	2
Hrp1	CENP-A chaperone, CHD family Hrp1	SPAC1783.05	159	0	0	0	0	2
Mfs3	plasma membrane spermidine transmembrane transporter Mfs3	SPBC36.03c	59	11	0	0	0	2
Ght5	plasma membrane high-affinity glucose/fructose:proton symporter Ght5	SPCC1235.14	60	10	0	0	0	2
Rps1401	40S ribosomal protein S14	SPAC3H5.05c	15	0	0	0	0	2
Tif313	translation initiation factor eIF3m	SPAC1751.03	45	0	0	0	0	2
Erg2	C-8 sterol isomerase Erg2	SPAC20G8.07c	25	0	0	0	0	2
Pda1	pyruvate dehydrogenase e1 component alpha subunit Pda1	SPAC26F1.03	45	0	0	0	0	2
Rpl501	60S ribosomal protein L5	SPAC3H5.12c	33	0	0	0	0	2
rps002	40S ribosomal protein S0B	SPAPJ698.02c	31	0	0	0	0	2
Rpt4	19S proteasome base subcomplex ATPase subunit Rpt4	SPCC1682.16	44	0	0	0	0	2
SPCC126.08c	lectin family glycoprotein receptor	SPCC126.08c	35	1	0	0	0	2

Ifa38	ketoreductase involved in fatty acid elongation	SPAC4G9.15	37	1	0	0	0	2
Mug157	alpha-mannosidase GH125 family Mug157	SPAC12B10.16c	57	0	0	0	0	2
Cct8	chaperonin-containing T-complex theta subunit Cct8	SPBC337.05c	60	0	0	0	0	2
Rpl2801	60S ribosomal protein L27/L28	SPBC776.11	17	0	0	0	0	2
Cit1	citrate synthase Cit1	SPAC6C3.04	54	0	0	0	0	2
Elo2	fatty acid elongase Elo2	SPAC1B2.03c	38	6	0	0	0	2
Vht1	plasma membrane vitamin H transmembrane transporter Vht1	SPAC1B3.16c	63	12	0	0	0	2
Qcr9	ubiquinol-cytochrome-c reductase complex subunit 9	SPCC1682.01	8	1	0	0	0	2
Rpl702	60S ribosomal protein L7b involved in cytoplasmic translation	SPAC3H5.07	28	0	0	0	0	2
Gcv2	glycine cleavage complex subunit P	SPAC13G6.06c	114	0	0	3	0	0
Met10	sulfite reductase NADPH flavoprotein subunit	SPCC584.01c	111	0	0	2	0	0
Tif302	translation initiation factor eIF3b (p84)	SPAC25G10.08	84	0	0	2	0	0
Sum1	sum1, translation initiation factor eIF3i	SPAC4D7.05	37	0	0	2	0	0
Rpn2	19S proteasome regulatory subunit Rpn2	SPBC17D11.07c	107	0	0	2	0	0
